Performance of an Optical Relay Satellite Using Reed-Solomon Coding Over a Cascaded Optical PPM and BPSK Channel

D. Divsalar
Communications Systems Research Section

F. Naderi
Telecommunications Systems Section

The concept of using a relay satellite which receives information from deep space vehicles over an optical channel and relays this information to Earth over a microwave channel has been considered in the past. An important consideration in such a system is the nature of the optical/microwave interface aboard the relay satellite. In order to allow for the maximum system flexibility, without overburdening either the optical or RF channel, this paper considers the option of demodulating the optical channel on board the relay satellite but leaving the optical channel decoding to be performed at the ground station.

This not only removes some degree of complexity from the relay satellite but more importantly it circumvents restricting all deep space vehicles to a specific channel coding for which the decoder is provided on board the relay. For this scheme to be viable, the occurrence of erasures in the optical channel must be properly treated. A hard decision on the erasure (i.e., the relay selecting a symbol at random in case of erasure occurrence) seriously degrades the performance of the overall system. In this paper, we suggest coding the erasure occurrences at the relay and transmitting this information via an extra bit to the ground station where it can be used by the decoder. Many examples with varying bit/photon energy efficiency and for the noisy and noiseless optical channel have been considered. It is shown that coding the erasure occurrences dramatically improves the performance of the cascaded channel relative to the case of hard decision on the erasure by the relay.

I. Introduction

Optical communication systems have been studies in the past as a means of improving and/or expanding the capabilities of NASA's current Deep Space Network (Ref. 1). The principal advantage in communicating with optical frequencies is the potential increase in the information that can be transmitted to Earth from a deep space vehicle (DSV) having limited power and a structurally small antenna. However, Earth's atmosphere and adverse weather effects introduce attenuation and possible outages which limit the reliability of an Earth-based optical system.

In order to eliminate the atmospheric effects detrimental to optical links, an orbiting relay satellite might be employed. Such a satellite outside the Earth's atmosphere at the geosynchronous orbit would receive signals from the deep space vehicle over an optical link and subsequently relay the signals to Earth via a conventional microwave link (Ref. 2). Under this concept one would exploit advantages afforded by an optical link while eliminating some of its negative attributes. Figure 1 shows the block diagram for the optical/microwave communication system.

In the above, an important consideration is the nature of the optical/microwave link interface. Two alternatives were discussed in an earlier report (Ref. 2) and are briefly discussed here. Figure 2 shows the interface for option 1. Here the output of the photodetector is demodulated and decoded to recover the baseband data, which then modulates an RF carrier prior to transmission to Earth. The overall bit error probability at the ground station is given by the expression

$$PE = PE_{RF} + PE_o - 2PE_{RF}PE_o \approx PE_{RF} + PE_o \qquad (1)$$

where PE_{RF} and PE_o are the bit error probabilities in the microwave and optical links respectively. The principal disadvantage of this scheme, which we shall refer to as a "demodulate and decode," is that by placing the demodulator and the decoder on the relay, the system is dictating the modulation and channel coding schemes to be used by all deep space vehicles which want to communicate through the relay satellite.

To mitigate this problem, the satellite can be operated in the "bent pipe" mode. Figure 3 shows the optical/microwave interface for this option where the analog output of the photodetector, $x(t)$, directly modulates (e.g., FM) an RF carrier. At the ground station, the RF carrier is demodulated to get an estimate of $x(t)$, which is then routed to an optical demodulator and a channel decoder to recover the baseband data. While this scheme offers the most flexibility, it also imposes a wide bandwidth requirement on the microwave link. The performance of this system is being studied.

As a compromise between the above two alternatives, a third option is discussed and evaluated in this paper. In order to eliminate the wide bandwidth requirement of the bent pipe option and yet retain some degree of flexibility in the system, consider the case where the output of the photodetector on the relay satellite is demodulated but not decoded. The demodulated bit stream modulates an RF carrier for transmission to the ground station where the carrier is demodulated and decoded to recover the baseband data.

As an example, the optical link may use Reed-Solomon (RS) coding followed by a pulse position modulation (PPM) to transmit data from deep space to the relay satellite where the received signal is demodulated and the ensuing bit stream modulates an RF carrier using binary phase shift keying (BPSK). In the next section we analyze the performance of this system.

II. Performance of Reed-Solomon Coding Over Cascaded Optical PPM and BPSK Channel

In this section we analyze the performance of an (N, K) RS code over cascaded M-ary optical PPM and binary PSK channels. The mathematical model for the system under consideration is shown in Fig. 4. Allowing for erasure, the PPM channel can be modeled as an M-ary input $(M+1)$-ary output discrete memoryless channel (DMC), characterized by symbol error probability P_s, erasure probability P_e and correct symbol probability P_c, shown in Fig. 5.

Two cases are considered. In the first case the erasure is eliminated on the relay satellite by hard decision (i.e., a symbol is randomly selected in case of an erasure occurrence). In the second case, the occurrence of an erasure is properly coded and transmitted to the ground station where this information is used by the decoder.

Case A — Hard Decision on Erasures at the Relay

In the case of hard decision, the symbol error probability P_{sh} and correct symbol probability P_{ch} are given by

$$P_{sh} = P_s + \frac{M-1}{M} P_e \qquad (2)$$

and

$$P_{ch} = P_c + \frac{1}{M} P_e \qquad (3)$$

After PPM demodulation (and the hard decision) RS symbols must be sent over a binary symmetric channel (BSC) characterized by bit error probability P_b given as

$$P_b = 1/2 \text{ erfc } \left(\sqrt{\frac{E_b}{N_0}}\right) \tag{4}$$

where E_b is energy per bit and N_0 is the one-sided noise spectral density at the ground station. Since each RS symbol can be represented by $n = \log_2 M$ bits, transmission of an RS symbol can be modeled by a $(BSC)^n$ channel as depicted in Fig. 6.

The equivalent cascaded M-ary PPM channel, with hard-decided erasure symbols, and $(BSC)^n$ channel is shown in Fig. 7. From this figure, the symbol error probability of the equivalent channel is given by

$$\pi_{sh} = 1 - \left[\left(1 - \frac{MP_{sh}}{M-1}\right) (1-P_b)^n + \frac{P_{sh}}{M-1}\right] \tag{5}$$

If an (N, K) RS code is used in conjunction with the cascaded channel, a word error occurs when there are more than $(N-K)/2$ symbol errors in the N symbol received code word; then the word error probability of the RS code is given by

$$P_{wh}(RS) = \sum_{k=\frac{N-K}{2}+1}^{N} \binom{N}{k} \pi_{sh}^k (1-\pi_{sh})^{N-k} \tag{6}$$

where $N = M - 1$. Note that for large alphabet size RS codes in which we are interested, since the mass of spheres (with radius of one-half of the code minimum distance) around the code words is much smaller than the mass of total signal space, for a practical range of bit error rates, the probability of an incorrect decoding event can be ignored. Thus when the RS code fails to decode, we may have a bit in error. Under these conditions a bit error occurs when a bit in a received symbol is in error and there are $(N-K)/2$ or more symbol errors in the remaining $N-1$ symbols in a received code word. Then the bit error rate of the RS code is given by

$$P_{bh}(RS) = \left[\frac{M\pi_{sh}}{2(M-1)}\right] \sum_{k=\frac{N-K}{2}}^{N-1} \binom{N-1}{k} \pi_{sh}^k (1-\pi_{sh})^{N-1-k} \tag{7}$$

In (7), the expression in brackets represents the bit error probability before RS decoding and the summation in (7) represents the probability of making $(N-K)/2$ or more symbol errors in $N-1$ symbols of received code word.

Case B — No Hard Decision on Erasures at the Relay

We now consider the case where erasure information is encoded and relayed to the ground station and compare the performance with that of hard-decided erasure on the relay.

In order to transmit the erasure symbols over the downlink BSC, an extra bit is appended to the RS symbols. (We shall see shortly that for the range of E_b/N_0 of interest, one extra bit is sufficient to achieve acceptable performance). This means that symbols sent over the BSC channel are of lengths $n+1$ bits. At the ground station the decoder examines the $(n+1)th$ bit; if it is zero, the decoder accepts the first n bits as the RS symbol. However, if the appended bit is one, the receiver declares an erasure symbol and disregards the first n bits. For this case for each transmission of RS or erasure symbols the channel can be modelled as $(BSC)^{n+1}$. The equivalent cascaded PPM and $(BSC)^{n+1}$ channel is shown in Fig. 8. From this figure, the symbol erasure probability of the equivalent channel is:

$$\pi_e = P_c P_b + P_s P_b + P_e (1-P_b) \tag{8}$$

and the symbol error probability is

$$\pi_s = P_c [1-(1-P_b)^n] (1-P_b) + \frac{M-1}{M} P_e P_b + \frac{1}{M-1} P_s [M-2+(1-P_b)^n] (1-P_b) \tag{9}$$

While the correct symbol probability is

$$\pi_c = P_c (1-P_b)^{n+1} + \frac{1}{M} P_e P_b + \frac{1}{M-1} P_s \cdot [1-(1-P_b)^n] (1-P_b) \tag{10}$$

From the above three equations, the word error and the bit error probability of the RS code over the equivalent channel of Fig. 8 are given by (Ref. 3).

$$P_{ws}(RS) = \sum_{i=0}^{N} \sum_{j=\Delta}^{N-i} \binom{N}{i} \binom{N-i}{j} \pi_s^i \pi_e^j \pi_c^{N-i-j} \tag{11}$$

and

$$P_{bs}(RS) = \frac{M}{2(M-1)} \sum_{i=0}^{N} \sum_{j=\Delta}^{N-i} \binom{N}{i} \binom{N-i}{j} \frac{i+j}{N} \cdot \pi_s^i \, \pi_e^j \, \pi_c^{N-i-j} \tag{12}$$

where

$$\Delta = MAX\,(N-K+1-2i, 0) \tag{13}$$

III. Numerical Results

In order to compare the performance of the two cases discussed in the previous section, we now consider specific examples. Consider using M-ary PPM with $M = 256$ and three RS codes, namely (255, 223), (255, 191) and (255, 127).

Both noisy and noiseless optical channels are considered. Assuming no background noise, the PPM channel can be viewed as a purely erasure channel with

$$P_e = e^{-K_s} \tag{14}$$

and

$$P_c = 1 - e^{-K_s} \tag{15}$$

where K_s is the average number of photon counts per PPM frame of the optical channel. For the case of hard-decided erasures, using Eqs. (14) and (15) above in Eqs. (2) and (3) with P_s set to zero, we have

$$P_{sh} = \frac{M-1}{M} e^{-K_s} \tag{16}$$

and

$$P_{ch} = 1 - \frac{M-1}{M} e^{-K_s} \tag{17}$$

Using these results, we have plotted the bit error rate of the end-to-end system (i.e., $P_{bh}(RS)$) for the hard-decided erasure from Eq. (7) and $P_{bs}(RS)$ for the coded erasure from Eq. (12) as a function of E_b/N_0 of the microwave channel for various energy efficiency of ρ bits/photon where ρ is given by

$$\rho = \frac{K \log_2 M}{N K_s} \tag{18}$$

The results are given in Figs. 9-11.

Next the procedure is repeated for the case of a noisy optical channel. In the presence of background noise, a PPM threshold detector (Ref. 3) is used where for each slot in the PPM frame, the number of received photons is compared with a threshold γ to decide the presence or the absence of the signal.

Assume Poisson distribution on the number of received photons in each slot, with a mean K_b in the absence of the signal and mean $K_b + K_s$ in the presence of a signal in the slot. Then the probability of correctly detecting the presence of the signal is given by

$$P_{ds} = \sum_{k=\gamma+1}^{\infty} \frac{(K_s + K_b)^k}{k!} e^{-(K_s+K_b)} \tag{19}$$

and the probability of correctly detecting the absence of the signal (or presence of the noise) is given by

$$P_{dn} = \sum_{k=0}^{\gamma} \frac{(K_b)}{k!} e^{-K_b} \tag{20}$$

Using Eqs. (19) and (20) we have

$$P_s = (M-1)(1-P_{ds})(1-P_{dn}) P_{dn}^{M-2}$$

$$P_c = P_{ds} P_{dn}^{M-1} \tag{21}$$

$$P_e = 1 - P_c - P_s$$

These results are next used in Eqs. (2) and (3) to calculate P_{sh} and P_{ch} and in Eqs. (8) through (10) to calculate π_e, π_s and π_c, which are subsequently used to calculate $P_{bh}(RS)$ and $P_{bs}(RS)$. The threshold γ has been optimized to give minimum bit error rates. $P_{bh}(RS)$ and $P_{bs}(RS)$ are shown in Figs. 12-20.

IV. Conclusion

This paper has considered an optical relay satellite system which has been modeled as a cascaded optical PPM and microwave BPSK channel. In order to maintain maximum system flexibility, the relay satellite demodulates but does not decode the optical channel; the decoding is performed by the ground station. The occurrence of optical erasures is properly coded by the relay and transmitted to the ground decoder using an extra bit. It is shown that this improves the overall system performance dramatically relative to the case where the relay makes hard decision on the erasures, thereby screening the ground decoder from the knowledge of such erasure occurrences.

References

1. Vilnrotter, V. A., and Gagliardi, R. M., "Optical-Communication Systems for Deep Space Applications," Publication 80-7, Jet Propulsion Laboratory, Pasadena, California, March 15, 1980.

2. Gagliardi, R. M., Vilnrotter, V. A., and Dolinar, S. J., "Optical Deep Space Communication via Relay Satellite," Publication 81-40, Jet Propulsion Laboratory, Pasadena, California, August 15, 1981.

3. Lesh, J. R., Katz, J., Tan, H. H., and Zwillinger, D., "2.5-Bit/Detected Photon Demonstration Program: Analysis and Phase I Results," TDA Progress Report 42-66, Jet Propulsion Laboratory, Pasadena, California, pp. 115-132, December 15, 1981.

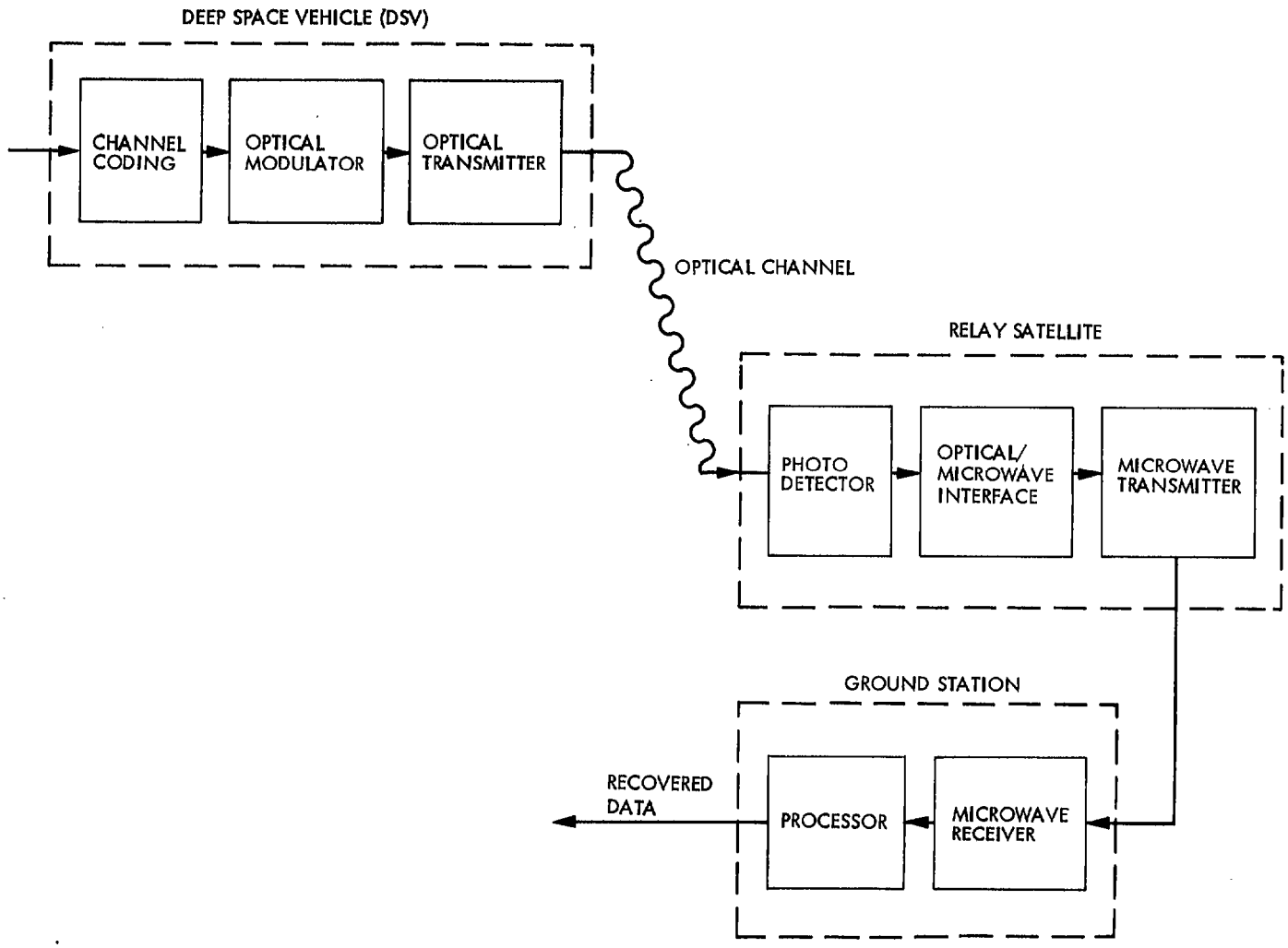

Fig. 1. Block diagram of an optical relay satellite system

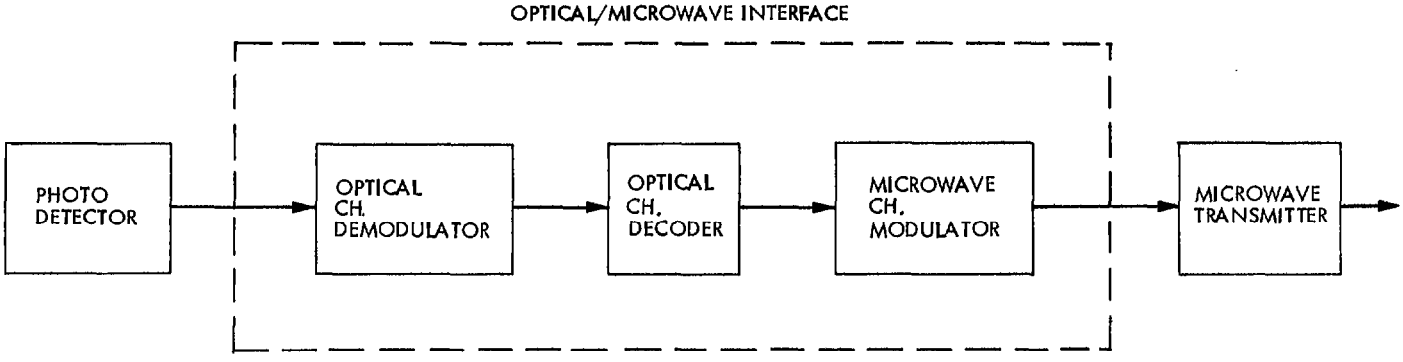

(a)
OPTICAL/MICROWAVE INTERFACE ON THE RELAY SATELLITE

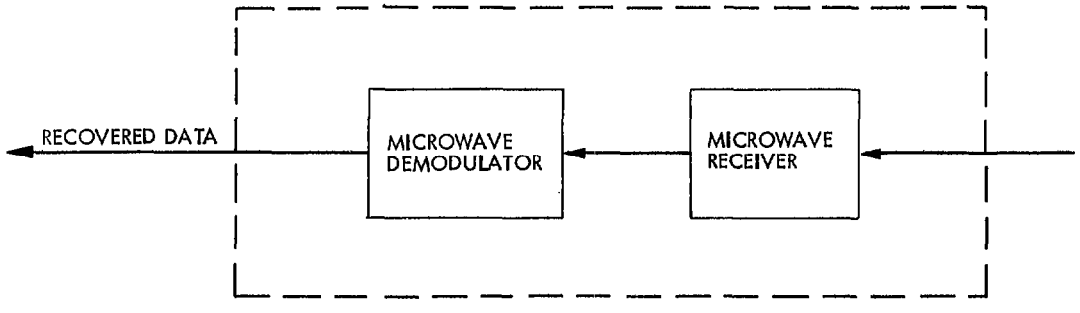

(b)
GROUND STATION PROCESSING

Fig. 2. Block diagram of "demodulate and decode" option

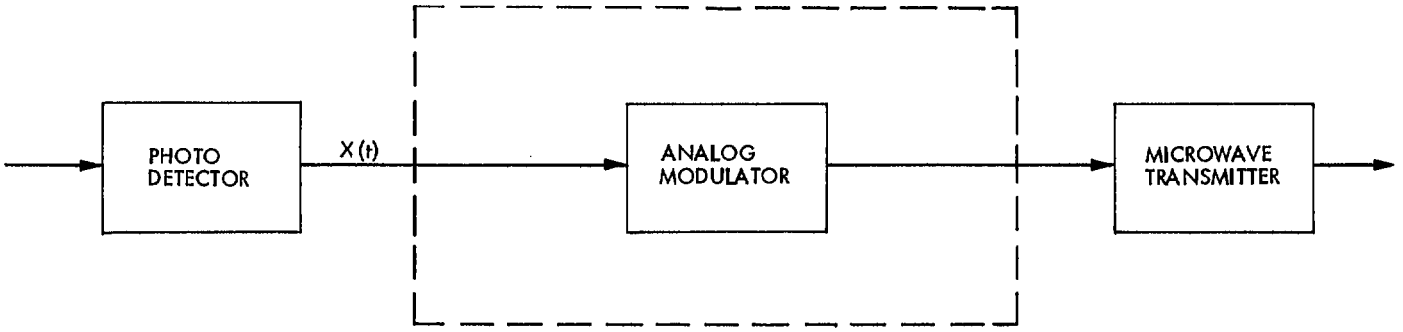

(a)
OPTICAL/MICROWAVE INTERFACE ON THE RELAY SATELLITE

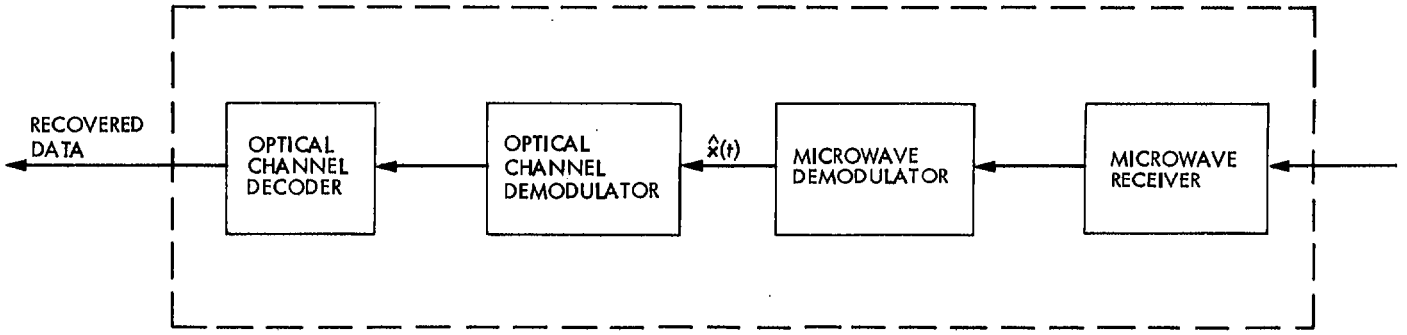

(b)
GROUND STATION PROCESSING

Fig. 3. Block diagram of the "bent pipe" option

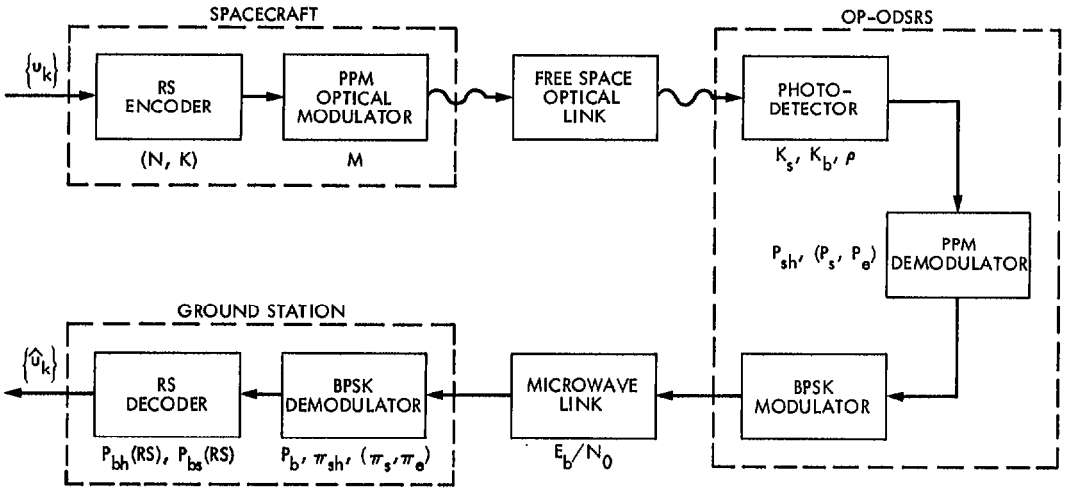

Fig. 4. Block diagram of the end-to-end system

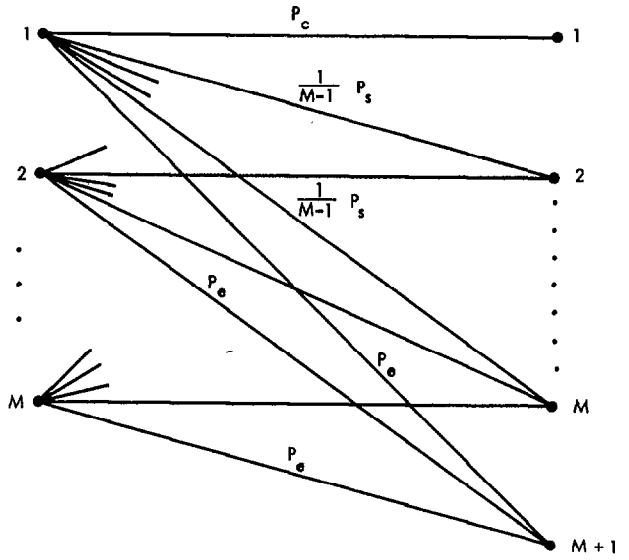

Fig. 5. PPM channel with erasure

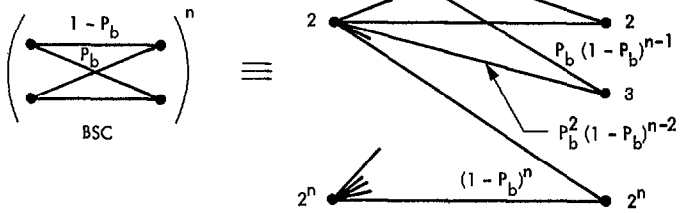

Fig. 6. $(BSC)^n$ channel

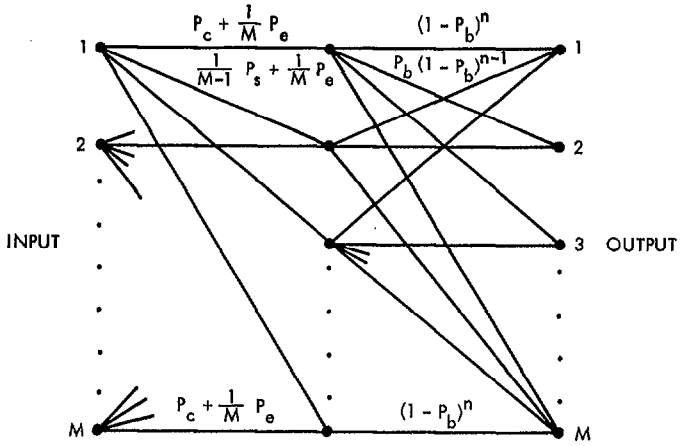

Fig. 7. Equivalent hard-decided cascaded channel

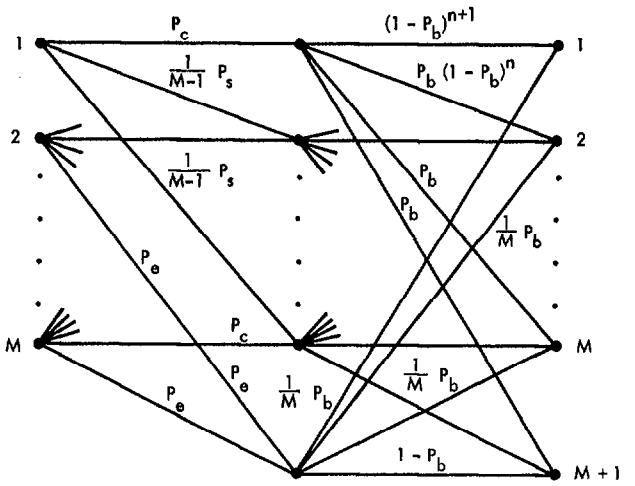

Fig. 8. Equivalent soft-decided cascaded channel (sending one extra bit for erasure symbol)

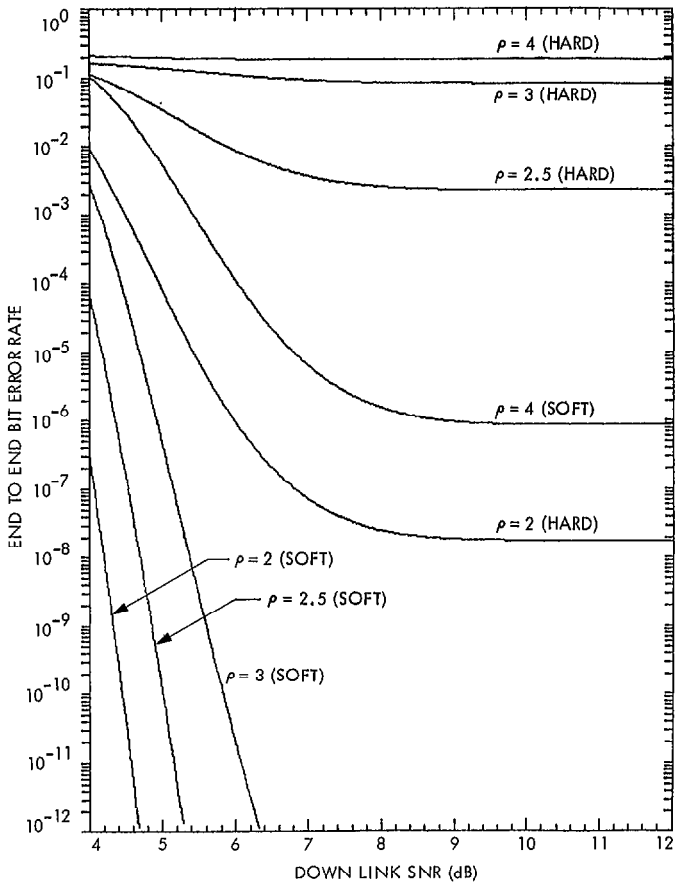

Fig. 9. P_{bh} (RS) and P_{bs} (RS) vs downlink E_b/N_0 for RS(255, 127), code rate ≈ 1/2 with no background noise, for various energy efficiency ρ (bits/photon)

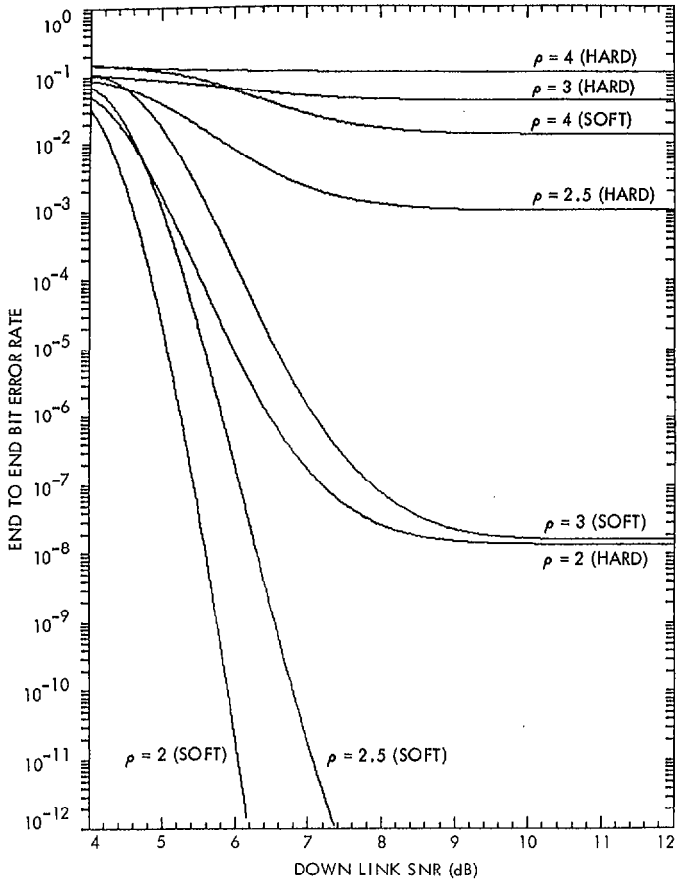

Fig. 10. P_{bh} (RS) and P_{bs} (RS) vs downlink E_b/N_0 for RS(255, 191), code rate ≈ 3/4 with no background noise, for various energy efficiency ρ (bits/photon)

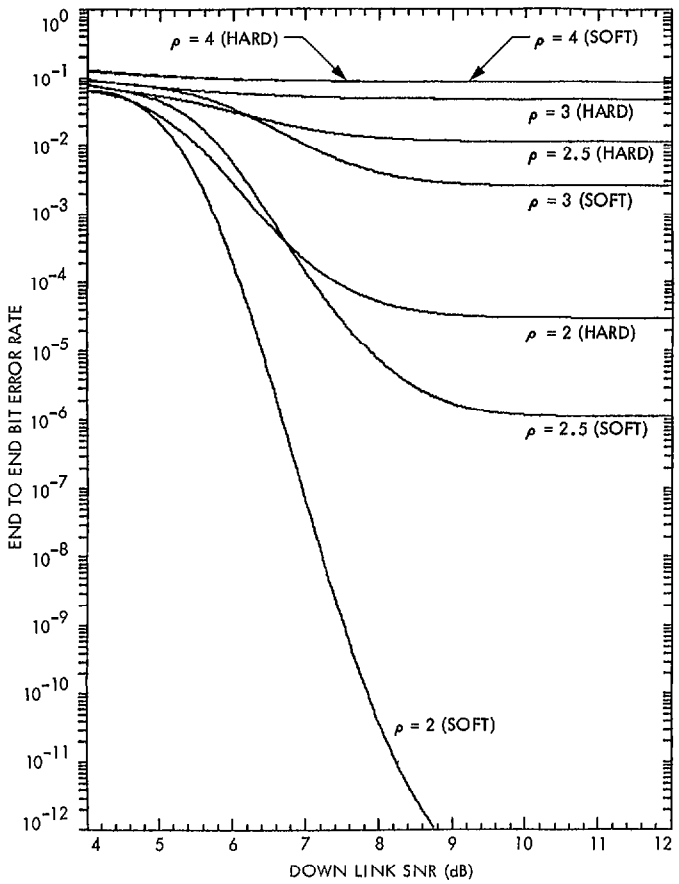

Fig. 11. P_{bh} (RS) and P_{bs} (RS) vs downlink E_b/N_0 for RS(255, 223), code rate ≈ 7/8 with no background noise, for various energy efficiency ρ (bits/photon)

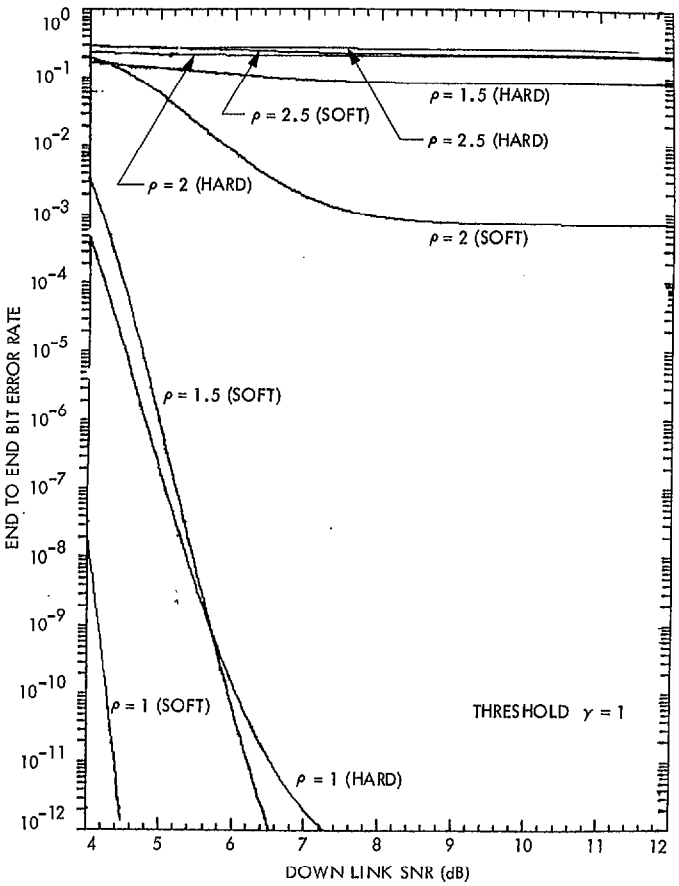

Fig. 12. P_{bh} (RS) and P_{bs} (RS) vs downlink E_b/N_0 for RS(255, 127), code rate ≈ 1/2 with background noise $K_b = 10^{-2}$, for various energy efficiency ρ (bits/photon)

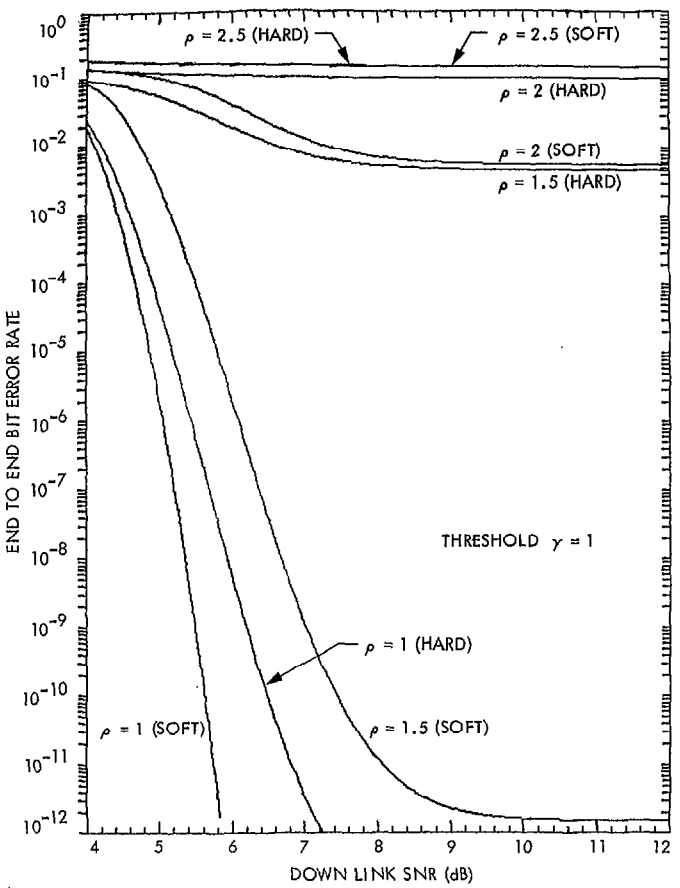

Fig. 13. P_{bh} (RS) and P_{bs} (RS) vs downlink E_b/N_0 for RS(255, 191), code rate ≈ 3/4 with background noise $K_b = 10^{-2}$, for various energy efficiency ρ (bits/photon)

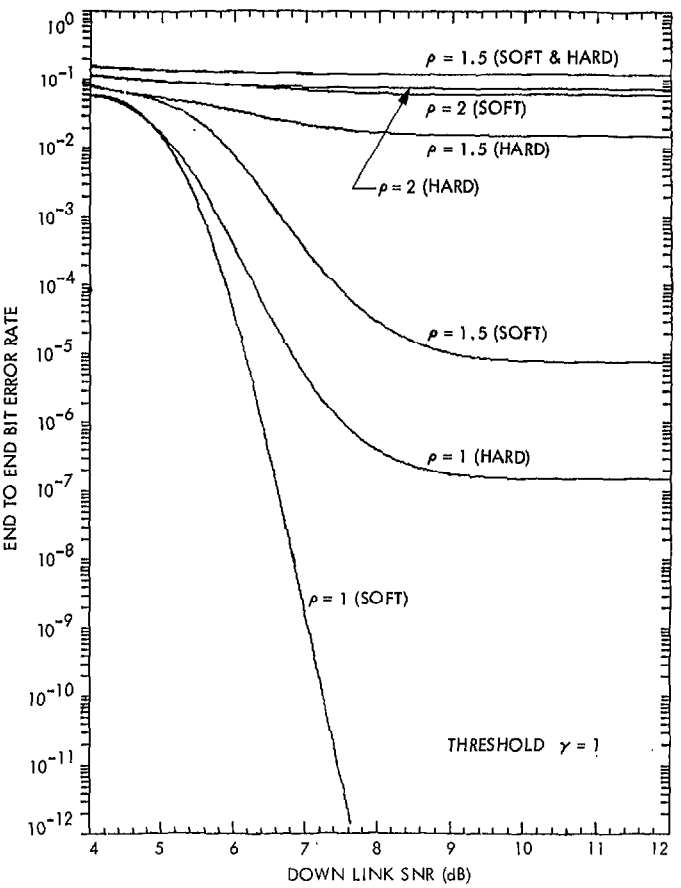

Fig. 14. P_{bh} (RS) and P_{bs} (RS) vs downlink E_b/N_0 for RS(255, 223), code rate ≈ 7/8 with background noise $K_b = 10^{-2}$, for various energy efficiency ρ (bits/photon)

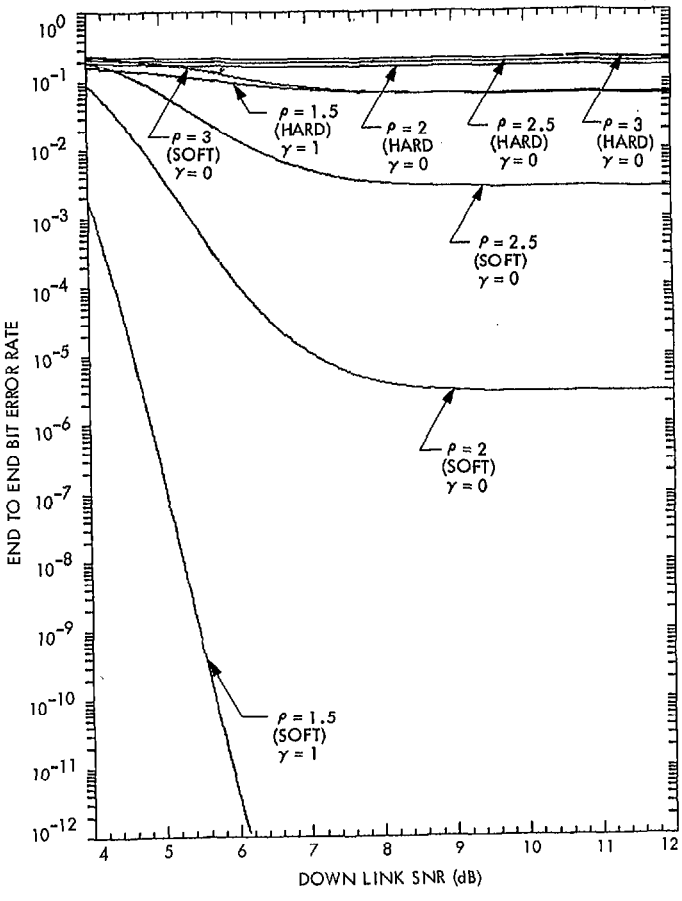

Fig. 15. P_{bh} (RS) and P_{bs} (RS) vs downlink E_b/N_0 for RS(255, 127), code rate ≈ 1/2 with background noise $K_b = 10^{-3}$, for various energy efficiency ρ (bits/photon)

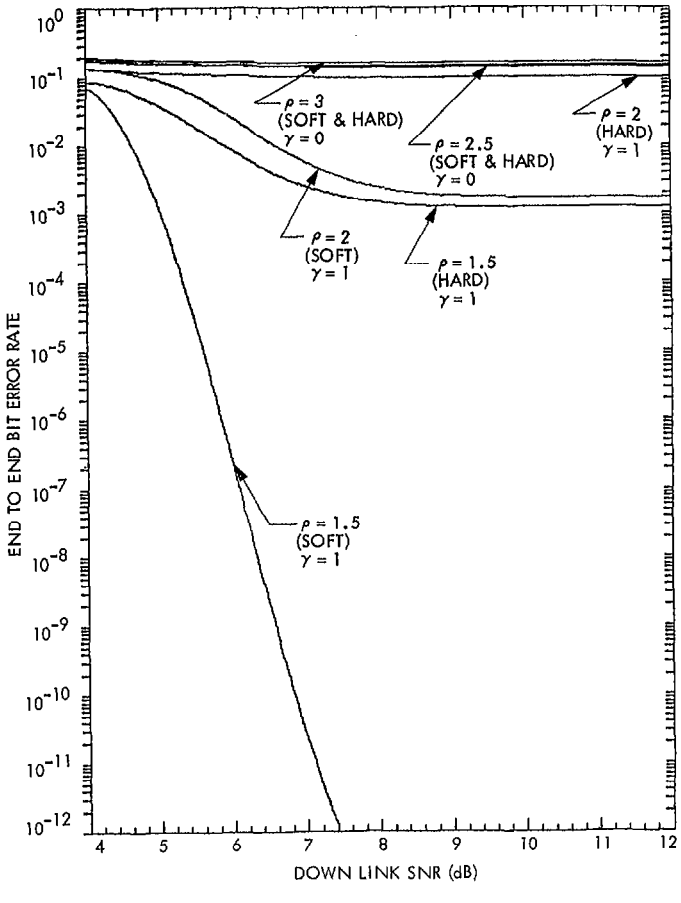

Fig. 16. P_{bh} (RS) and P_{bs} (RS) vs downlink E_b/N_0 for RS(255, 191), code rate ≈ 3/4 with background noise $K_b = 10^{-3}$, for various energy efficiency ρ (bits/photon)

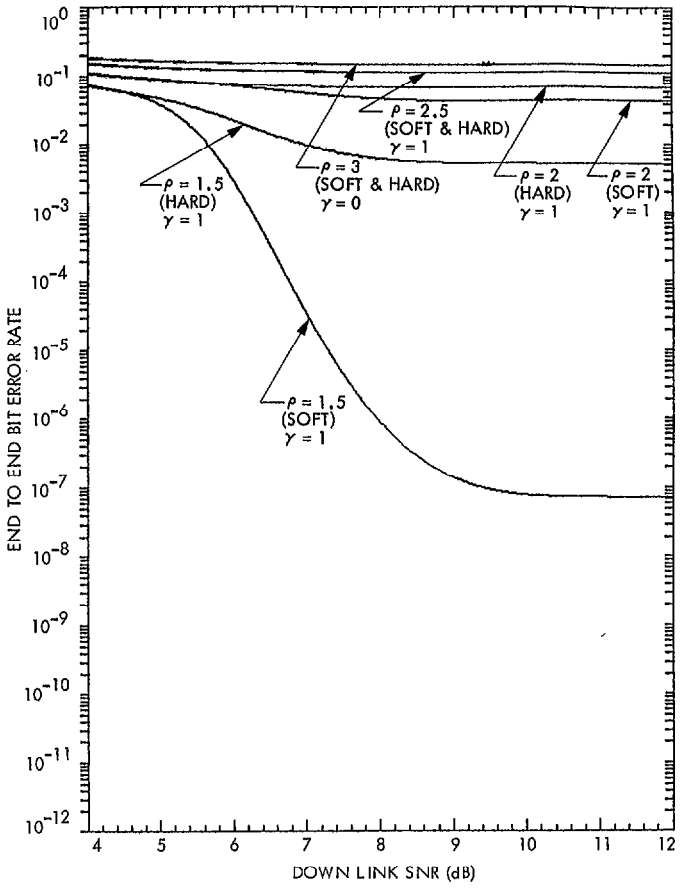

Fig. 17. P_{bh} (RS) and P_{bs} (RS) vs downlink E_b/N_0 for RS(255, 223), code rate ≈ 7/8 with background noise $K_b = 10^{-3}$, for various energy efficiency ρ (bits/photon)

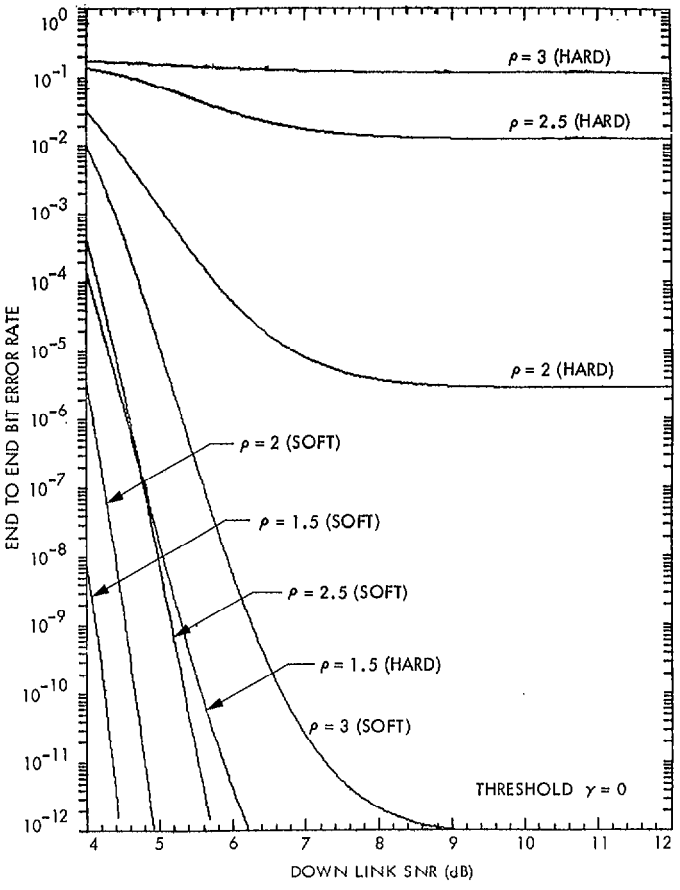

Fig. 18. P_{bh} (RS) and P_{bs} (RS) vs downlink E_b/N_0 for RS(255, 127), code rate ≈ 1/2 with background noise $K_b = 10^{-4}$, for various energy efficiency ρ (bits/photon)

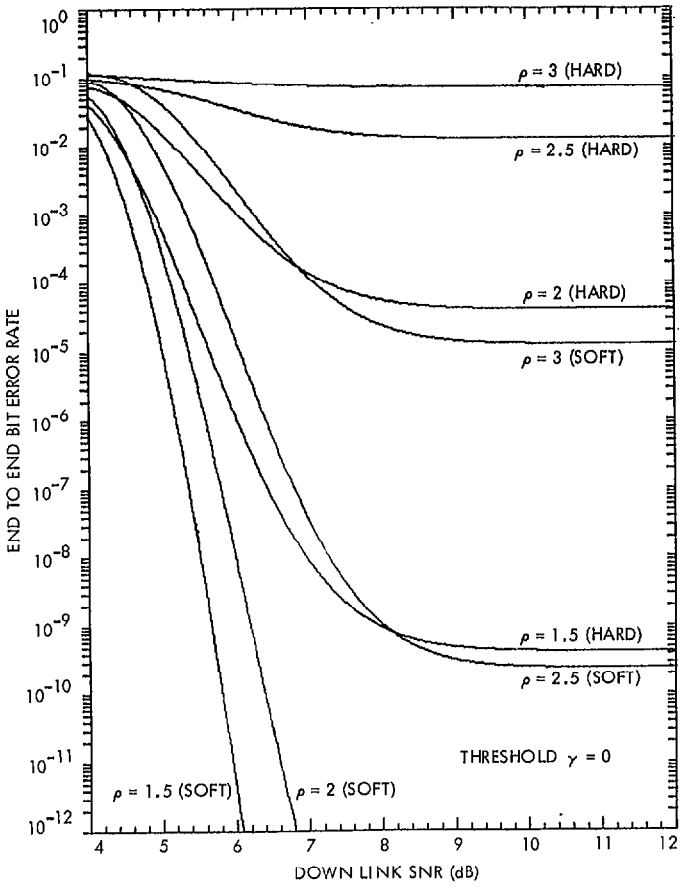

Fig. 19. P_{bh} (RS) and P_{bs} (RS) vs downlink E_b/N_0 for RS(255, 191), code rate ≈ 3/4 with background noise $K_b = 10^{-4}$, for various energy efficiency ρ (bits/photon)

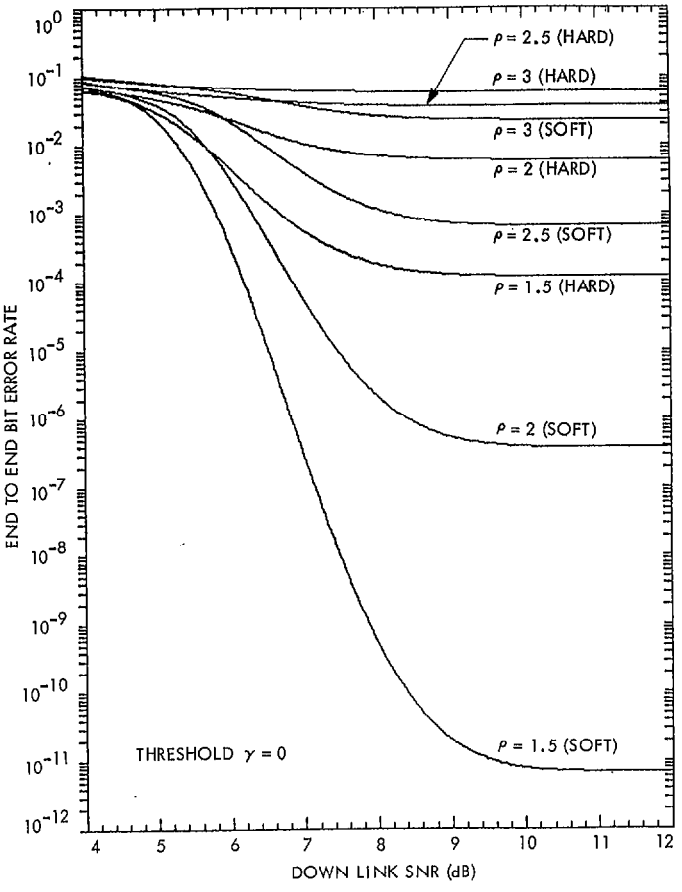

Fig. 20. P_{bh} (RS) and P_{bs} (RS) vs downlink E_b/N_0 for RS(255, 223), code rate ≈ 7/8 with background noise $K_b = 10^{-4}$, for various energy efficiency ρ (bits/photon)